Hydridosilicate σ-Complexes

DOI: 10.1002/anie.201202328

Stabilization of $ArSiH_4^-$ and SiH_6^{2-} Anions in Diruthenium Si–H σ-Complexes**

*Mark C. Lipke and T. Don Tilley**

Transition-metal centers are known to stabilize a wide variety of highly reactive species,[1,2] and this is often attributed to the presence of strong d_π-back-donation from the metal to formally empty π-symmetry orbitals on the ligated species.[3] Many unsaturated silicon species can be stabilized in this way, and examples include silylene,[2b,c] silene,[2d,e] disilene,[2f,g] and silabenzene[2h,i] complexes. The transition-metal stabilization of saturated, reactive species as σ-complexes is less common, but examples involving hypercoordinate silicon centers have recently been reported, such as the hydridosilicate σ-complexes $L_nM[\eta^3\text{-}H_2SiR_3]$ (R = H, alkyl, aryl, Cl; L_nM = CpFe(P*i*Pr_2Me),[4a] TpRu(PPh_3)[4b]). Related metal complexes of the type $L_3MH_3SiR_3$ (M = Fe, Ru, Os, L = R_3P, H_2, CO) may possess significant $[L_3M\{\eta^4\text{-}H_3SiR_3\}]$ character,[5] but these have more typically been described as silyl complexes[6a–d] or η^2-$HSiR_3$[6e] σ-complexes with additional secondary Si···H interactions.[6] It is interesting that transition metals can participate in the formation and stabilization of hydridosilicate anions since these anions are usually highly reactive and have most often been studied as transient intermediates[7] or in the gas phase.[8] The few examples of $[HSiR_4]^-$ and $[H_2SiR_3]^-$ salts (R = Ar, OR, F) that have been isolated are highly reactive,[9] and transition-metal complexes of these anions may also exhibit interesting reactivity.[4b] Given the unusual structures of hydridosilicate σ-complexes and their potential role in metal-mediated transformations, it is important to more fully develop the chemistry of these hypercoordinate silicon species.

We recently reported unusual silane σ-complexes $[\{PhBP^{Ph}_3\}RuH(\eta^3\text{-}H_2SiRR')]$ (RR′ = Me,Ph **2a**; RR′ = Ph_2 **2b**) that feature formal donation of two Si–H bonds to ruthenium. These compounds were obtained by reaction of secondary silanes with $[\{(PhBP^{Ph}_3)Ru(\mu\text{-}Cl)\}_2]$ (**1**), as illustrated by the synthesis of complexes **2a,b** (Scheme 1). These complexes are highly electrophilic at silicon, and readily add Lewis bases to form $[\{PhBP^{Ph}_3\}Ru\{(\mu\text{-}H)_3SiRR'(base)\}]$ complexes with hypercoordinate silicon centers.[10] Similar chemistry has proven difficult to extend to primary silanes ($RSiH_3$), which might be expected to produce reactive

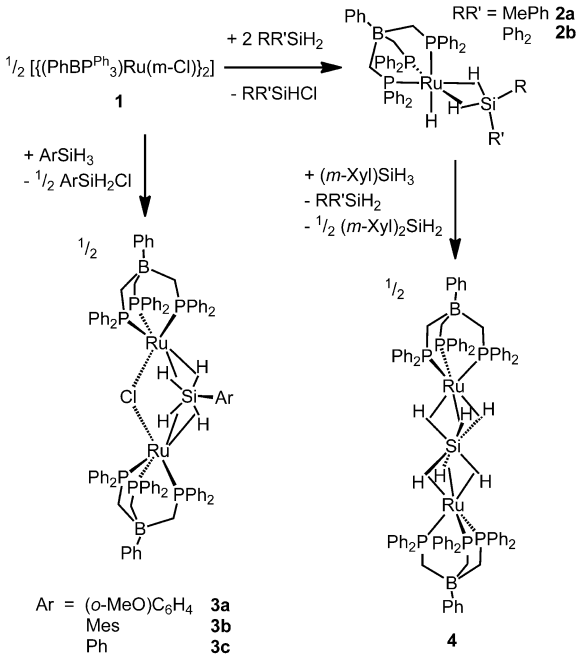

Scheme 1. Syntheses of complexes **2a–b**, **3a–c**, and **4** starting from **1**.

complexes of the type $[\{PhBP^{Ph}_3\}RuH(\eta^3\text{-}H_2Si(H)R)]$. Efforts to prepare such compounds have included the examination of reactions of arylsilanes $ArSiH_3$ (Ar = 2-$MeOC_6H_4$, Mes, Ph) with **1**, which instead produced highly unusual hydridosilicate σ-complexes $[\{(PhBP^{Ph}_3)Ru\}_2(\mu\text{-}Cl)\{\mu\text{-}\eta^3,\eta^3\text{-}H_4SiAr\}]$ (Ar = 2-$MeOC_6H_4$, **3a**; Mes, **3b**; Ph, **3c**; Scheme 1), as described below. Furthermore, displacement of Ph_2SiH_2 from **2** with (*m*-Xyl)SiH_3 or SiH_4 results in formation of $[\{(PhBP^{Ph}_3)Ru\}_2\{\mu\text{-}\eta^4,\eta^4\text{-}H_6Si\}]$ (**4**; Scheme 1), a diruthenium complex with the novel η^4,η^4-$[H_6Si]^{2-}$ ligand.

Treatment of **1** with excess (2-$MeOC_6H_4$)SiH_3 (6 equiv) in C_6D_6 resulted in quantitative formation of **3a** (by ^1H and $^{31}P\{^1H\}$ NMR spectroscopy) and 1 equiv of (2-$MeOC_6H_4$)SiH_2Cl (^1H NMR: $\delta = 5.36$ ppm, $^1J_{SiH} = 242$ Hz) within 30 min.[11] Compound **3a** spontaneously crystallized from this solution after 24 h, and single-crystal X-ray diffraction was used to determine a dinuclear structure featuring a (2-$MeOC_6H_4$)Si fragment that bridges the two ruthenium centers, but the hydride ligands could not be located (Figure 1a). Multinuclear NMR data for **3a** (CD_2Cl_2) are consistent with a dinuclear structure that includes the $[(2\text{-}MeOC_6H_4)SiH_4]^-$ anion. The 2-$MeOC_6H_4$ group is present in a 1:2 ratio with the $[PhBP^{Ph}_3]^-$ ligand, and the two $\{[PhBP^{Ph}_3]Ru\}$ fragments are equivalent in the $^{31}P\{^1H\}$ NMR spectrum of **3a**, which displays three triplet resonances ($^2J_{PP}$ =

[*] M. C. Lipke, Prof. T. D. Tilley
Department of Chemistry, University of California, Berkeley
Berkeley, CA 94720-1460 (USA)
E-mail: tdtilley@berkeley.edu

[**] Support for this research was provided by The National Science Foundation under Grant No. CHE-0957106. Support for the Molecular Graphics and Computational Facility is provided by the National Science Foundation under Grant No. CHE-0840505.

Supporting information for this article is available on the WWW under http://dx.doi.org/10.1002/anie.201202328.

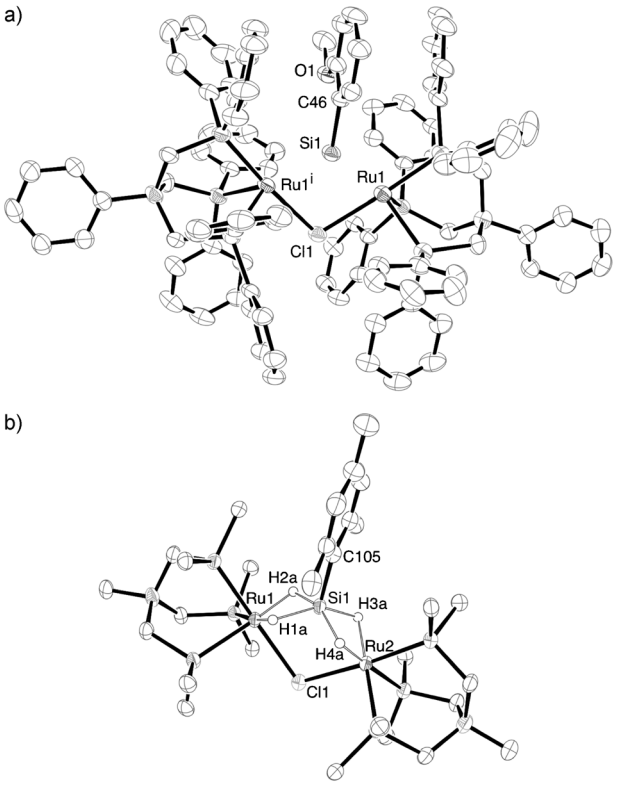

Figure 1. a) Structure of **3a** determined by single-crystal X-ray diffraction analysis (XRD; ellipsoids set at 50% probability).[30] The OMe group is disordered equally between two positions that are related by a C_2 rotation about the Si–C46 axis. Only one orientation of the OMe group is shown, and hydrogen atoms are omitted for clarity. Si1–Ru1 2.3337(9) Å. b) Structure of **3b** determined by single crystal XRD (ellipsoids set at 50% probability).[30] Non-hydridic hydrogen atoms and non-*ipso* phenyl carbon atoms have been omitted for clarity. Selected bond lengths [Å] and angles [°]: Si1–H1a 1.62(4), Si1–H2a 1.68(3), Si1–H3a 1.66(4), Si1–H4a 1.66(3), Si1–C105 1.871(4), Si1–Ru1 2.3659(9), Si1–Ru2 2.3599(9); H1a-Si1-H2a 84(2), H1a-Si1-H4a 87(2), H2a-Si1-H3a 86(2), H3a-Si1-H4a 88(2), C105-Si1-H1a 106(1), C105-Si1-H2a 104(1), C105-Si1-H3a 107(1), C105-Si1-H4a 104(1).

36 Hz, $\delta = 49.6$, 30.6, 30.0 ppm). Two ^{1}H NMR resonances, each integrating as two hydride ligands, appear near −5 ppm. The slight inequivalence of the hydride resonances is attributed to the orientation of the *o*-anisyl group. Hindered rotation of the Si–Ar bond in **3a** may be expected based on steric interactions of the *o*-anisyl group with the [PhBP$^{Ph}_3$] ligand that are evident in the solid-state structure. The ^{1}H–^{29}Si HMBC NMR spectrum has a ^{29}Si resonance at 122 ppm that exhibits similar coupling constants for the two hydride resonances (^{1}H $\delta = -4.87$, −5.11 ppm; $J_{SiH} = 84$, 77 Hz). These J_{SiH} values are quite large and indicate that the hydride ligands engage in non-classical Ru–H–Si interactions.[12] The Ru–H signals exhibit coalescence at −80 °C in the ^{1}H NMR spectrum and are separated into three broad, partially overlapping resonances at −90 °C. The new Ru–H resonances (^{1}H $\delta = -4.60$ (2H), −5.41 (1H), −5.75 (1H)) feature chemical shifts that span a fairly narrow range, which suggests that all of the hydride ligands are in similar bonding environments. The FTIR spectra of **3a** feature a broad absorption centered at 1720 cm^{-1} for the solid (Nujol) or 1715 cm^{-1} in solution (CH_2Cl_2), which further indicates the presence of Ru–H–Si bonds that have a relatively strong Si–H bonding component (see below).[12b] Notably, the ^{29}Si chemical shift is downfield from the range observed for η^3-[H_2SiR_3]$^-$ σ-complexes (−13.8–70 ppm),[4] but is closer to the range observed for η^3-H_2SiR_2 σ-complexes (141–162 ppm).[10,13]

Treatment of **1** with an excess of $MesSiH_3$ (4 equiv) initially resulted in formation of a single product, which exhibited NMR data (^{31}P{^{1}H} $\delta = 45.7$ ppm; ^{29}Si $\delta = 108$ ppm; ^{1}H $\delta = -6.43$ ppm, Ru–H, $J_{SiH} = 82$ Hz, 3H) comparable to that of [{PhBP$^{Ph}_3$}RuH(η^3-H_2SiRR')] complexes.[10,13] This complex, presumed to be [{PhBP$^{Ph}_3$}RuH(η^3-$H_2SiClMes$)], could not be isolated but the slow transformation of this species to **3b** (50% yield), **4** (20% yield), and several minor products was evident by monitoring the reaction over one week by ^{1}H and ^{31}P{^{1}H} NMR experiments. Both **3b** and **4** crystallized from the reaction solution, which prevented the isolation of **3b** in pure form. The ^{1}H–^{29}Si HMBC NMR spectrum (using impure **3b**) revealed a ^{29}Si resonance at 116 ppm that was coupled to a hydride resonance at −4.95 ppm ($J_{SiH} = 82$ Hz). The Ru–H resonance for **3b** exhibits coalescence at −60 °C in the ^{1}H NMR spectum and at −90 °C is resolved into two doublets (^{1}H $\delta = -4.73$ (2H), −5.87 ppm (2H); $^2J_{PH} = 35.6$ Hz). A ^{29}Si-filtered ^{1}H-{^{31}P} NMR spectrum indicated large J_{SiH} values (>65 Hz) for each hydride resonance, but the signal-to-noise ratio was insufficient for determination of precise values. The variable-temperature NMR data for **3a,b** are consistent with the solid-state structures in which **3a** features C_1 symmetry (all four Ru–H resonances are inequivalent, but two overlap significantly) and **3b** features C_2 symmetry (two Ru–H resonances for 4 hydride ligands). Complex **3c** was similarly isolated with a small contaminant (10%) of **4** as an impurity, but it was identified by the similarity of its multinuclear NMR data to those of **3a,b** (**3c**: ^{29}Si $\delta = 120$ ppm, ^{1}H $\delta = -4.71$ ppm, Ru–H–Si $J_{SiH} = 80$ Hz).

The structure of **3b** (Figure 1b) was determined by X-ray diffraction analysis and is very similar to that of **3a**, but all hydride ligand positions were located and refined for **3b**. The Ru–Si distances (av. 2.3629(9) Å) are in the range typically observed for Ru–Si single bonds.[14] The silicon center features a five-coordinate, square-pyramidal geometry in which the mesityl group occupies the apical position and the hydrogen atoms occupy the basal positions. Related η^3-[H_2SiR_3]$^-$ complexes also feature a square-pyramidal geometry at silicon,[4] whereas free [$RSiH_4$]$^-$ anions are expected to exhibit a trigonal bipyramidal geometry.[15] Relatively short Si–H distances (<1.7 Å) indicate the presence of four coordinated Si–H bonds, which typically fall in a range from 1.50 Å (uncoordinated Si–H)[16] to 2.00 Å (full oxidative addition).[12a,b,17] It would require inaccuracy several times greater than the estimated standard deviation for the longest measured Si–H distance in **3b** (1.68(3) Å) to have a true value beyond this 2.00 Å limit. Systematic shortening of the M–H distance is a common error in determining hydride positions by XRD,[18] and this might influence the measured Si–H distances. However, this is not apparent for the measured Ru–H distances in **3b** (d(Ru–H)$_{3b}$ 1.58(4)–1.68(3) Å, av. 1.66(4) Å; d(Ru–H)$_{terminal}$ ca. 1.6 Å[19]). The structures of

3a,b were examined using DFT geometry optimization calculations (**3a**-DFT and **3b**-DFT),[20] which provided Si–H and Ru–H distances (dSi–H and dRu–H < 1.75 Å) that are slightly longer than those determined by XRD for **3b**, and fully consistent with coordinated Si–H bonds. Vibrational analysis of the optimized structures predicted a Ru–H stretching mode with a moderate IR intensity (1683.5 cm^{-1} for **3a**-DFT, 1695.3 cm^{-1} for **3b**-DFT) and weaker Ru–H absorptions at 1755.3 cm^{-1} (**3a**-DFT) and 1757.7 cm^{-1} (**3b**-DFT) that agree well with the broad Ru–H absorption observed at 1720 cm^{-1} in the FTIR spectrum for **3a**.

Notably, complexes **3a–c** exhibit no decomposition (determined by ^1H and ^{31}P NMR) after 1 week in CD_2Cl_2 at room temperature and are thus the most stable compounds containing an $[ArSiH_4]^-$ anion. The only previously isolated $[ArSiH_4]^-$ species $[Cp(iPr_2MeP)Fe(\eta^3\text{-}H_2SiPhH_2)]$ was reported to be unstable in solution,[4a] and related free $[RSiH_4]^-$ anions (R = H, alkyl, aryl) have only been studied by mass spectrometry and computational techniques.[8,15] Free hydridosilicate anions readily transfer hydride to other species (for example ketones and CO_2) in the gas phase,[8c,d] and this is attributed to the low hydride binding energies (hydride affinity, HA) of the parent silanes ($HA_{primary\,silane}$ = 16–22 kcal mol^{-1};[8c,d,15b] for comparison $HA_{benzene} = 21.5 \pm 4.2$ kcal mol^{-1}[21]). The remarkable stabilization of the $[ArSiH_4]^-$ anions in **3a–c** was examined by NBO and NLMO calculations,[22] which indicate that all four Ru–H–Si interactions are similar in nature (see the Supporting Information). Thus, the bis(η^3-H_2Si) coordination mode evenly removes electron density from all four electron-rich Si–H bonds such that none of the Si–H bonds are entirely broken. Note that the only previous examples of bis(η^3-H_2Si) coordination were reported for SiH_4 complexes $[\{(R_3P)_2H_2Ru\}_2(\eta^3,\eta^3\text{-}H_4Si)]$ (R = *i*Pr, Cy), in which substantial electron density is also withdrawn from silicon without cleavage of the Si–H bonds.[23]

The η^4,η^4-$[H_6Si]^{2-}$ complex **4** was formed in nearly quantitative yield by reaction of *m*-$XylSiH_3$ with **2b** in $[D_6]$benzene (by ^1H and $^{31}P\{^1H\}$ NMR; Scheme 1). The mild conditions and high yield for the formation of **4** are notable because the only previous synthesis of an $[SiH_6]^{2-}$ species involved extreme pressure and high temperature (> 4 GPa, > 450 °C) to convert KH, H_2, and elemental silicon into K_2SiH_6, which was detected as a minor constituent of the resulting mixture.[24] Complex **4** was isolated as a white powder in 34% yield and was characterized by NMR (CD_2Cl_2) and FTIR (Nujol, CH_2Cl_2) spectroscopy, as well as single-crystal XRD, making it the first $[SiH_6]^{2-}$ species to be isolated and characterized. All the phosphine ligands are equivalent (by $^{31}P\{^1H\}$ NMR spectroscopy) and there are three hydride ligands for each {[$PhBP^{Ph}_3$]Ru} moiety (by ^1H NMR spectroscopy). In the $^1H\{^{31}P\}$ NMR spectrum, the Ru–H resonance is a sharp singlet ($\delta = -6.41$ ppm) that features satellites from coupling to ^{29}Si ($J_{SiH} = 74.5$ Hz). This data is consistent with the η^4,η^4-$[H_6Si]^{2-}$ structure of **4**, but could also result from a less symmetric η^3,η^3-H_4Si structure $[\{(PhBP^{Ph}_3)RuH\}_2\{\mu\text{-}\eta^3,\eta^3\text{-}H_4Si\}]$ in which the terminal and bridging hydride positions exchange rapidly. The Ru–H resonance was broadened only slightly in the ^1H NMR spectrum collected at −90 °C, but the analogous exchange processes for **2a,b** are also rapid on the NMR timescale at −80 °C.[10] The ^1H–^{29}Si HMBC NMR spectrum of **4** has a ^{29}Si resonance (162 ppm) that is considerably upfield from that of $[\{(Cy_3P)_2H_2Ru\}_2(\eta^3,\eta^3\text{-}H_4Si)]$ (^{29}Si $\delta = 290$),[23] arguing against an η^3,η^3-H_4Si structure for **4**. It is interesting that **4** features an η^4,η^4-$[H_6Si]^{2-}$ ligand, unlike $[\{(R_3P)_2H_2Ru\}_2(\eta^3,\eta^3\text{-}H_4Si)]$, which instead exhibit a highly activated η^3,η^3-H_4Si ligand and terminal Ru–H bonds.[23] This difference suggests that *fac* η^4,η^4-coordination is important for stabilizing $[SiH_6]^{2-}$ in **4**, whereas the bulky *trans* phosphine ligands in $[\{(R_3P)_2H_2Ru\}_2(\eta^3,\eta^3\text{-}H_4Si)]$ make *fac* coordination of $[SiH_6]^{2-}$ less favorable.

In the reaction of **2b** with *m*-$XylSiH_3$, the formation of 1 equiv Ph_2SiH_2 and 0.5 equiv of $(m\text{-}Xyl)_2SiH_2$ was detected by ^1H NMR spectroscopy, and thus the formation of **4** appears to involve redistribution of (*m*-Xyl)SiH_3 to form $(m\text{-}Xyl)_2SiH_2$ and SiH_4. The reaction of SiH_4 with two equivalents of [{$PhBP^{Ph}_3$}RuH] would provide complex **4** by coordination of each Si–H bond to a ruthenium center and transfer of the two terminal hydride ligands to the electrophilic silicon atom.[10] Consistent with this mechanism, the addition of excess SiH_4 to a solution of **2** in $[D_6]$benzene resulted in the formation of **4** and release of Ph_2SiH_2 (by ^1H NMR spectroscopy; Eq. (1)). Furthermore, the redistribution of $PhMeSiH_2$

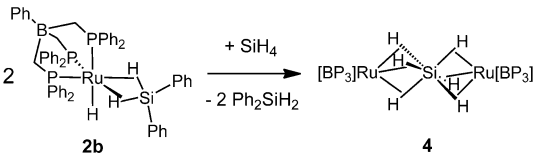

(1)

to Ph_2SiH_2, $PhMe_2SiH$, Ph_2MeSiH, Me_2SiH_2, and $MeSiH_3$ was observed by ^1H NMR spectroscopy after heating a solution of the silane and 10 mol% **2a** in $[D_6]$benzene to 60 °C for 20 h. Under these conditions, **2a** was converted into **4** in 90% yield, whereas only slight (< 5%) decomposition of **2a** to **4** was observed in the absence of $PhMeSiH_2$. Numerous transition-metal complexes mediate redistribution reactions of silanes, and several different mechanisms have been proposed and examined for such reactions.[25]

The FTIR spectra of **4** show a broad absorption at 1746 cm^{-1} (Nujol) or 1750 cm^{-1} (CH_2Cl_2), which is consistent with the Ru–H stretching mode of an Ru–H–Si interaction.[12b] Comparison of the FTIR data for **4** with that of related {[$PhBP^{Ph}_3$]Ru} complexes provides useful insight into the nature of the Ru–H–Si interactions. For example, the terminal Ru–H stretches for **2a,b** are at 1974 cm^{-1} (**2a**) and 1999 cm^{-1} (**2b**), while the Ru–H–Si bonds provide Ru–H stretches at lower wavenumber (1666 cm^{-1} **2a**; 1643 cm^{-1} **2b**). The 4-dimethylaminopyridine adducts of **2a,b** [{$PhBP^{Ph}_3$}Ru{$(\mu\text{-}H)_3SiRR'(DMAP)$}] (RR′ = MePh **2a**-DMAP; RR′ = Ph_2 **2b**-DMAP) show Ru–H stretches at 1883 cm^{-1} (**2a**-DMAP) and 1893 cm^{-1} (**2b**-DMAP). As the {[$PhBP^{Ph}_3$]Ru} fragment is constant amongst these species, the large differences in Ru–H stretching frequencies likely reflect the strength of the Si–H interactions. Thus, **4** appears to feature Ru–H–Si bonding in which the Si–H interactions are stronger than those in **2a,b**-

DMAP but weaker than those of the coordinated Si–H bonds in **2a,b**. The $^2J_{SiH}$ value for these compounds provides further support for this trend, with **4** exhibiting a J_{SiH} value (74.5 Hz) intermediate between those for the Ru–H–Si bonds of **2a,b** (ca. 100 Hz) and **2a,b**-DMAP (ca. 42 Hz).[10] Complex **3a** also features J_{SiH} values (77 Hz, 82 Hz) and a Ru–H stretching frequency (1720 cm^{-1}) that suggest Ru–H–Si interactions that are similar to those of **4**.

The structure of **4** was determined by XRD analysis using a crystal that was grown from a solution of **4** in toluene (**4**-tol; Figure 2a). The hydride positions revealed that **4** features an

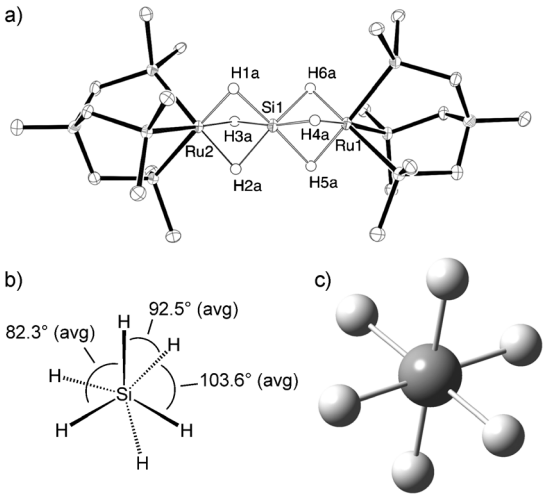

Figure 2. a) Structure of **4**-tol determined by single crystal XRD (ellipsoids set at 50% probability).[30] Non-hydridic hydrogen atoms, non-*ipso* phenyl carbon atoms, and three solvent molecules (toluene) were excluded for clarity. Selected bond lengths [Å]: Si1–H1a 1.75(3), Si1–H2a 1.77(4), Si1–H3a 1.69(4), Si1–H4a 1.69(3), Si1–H5a 1.76(4), Si1–H6a 1.79(4). b) Representation of the η^4:η^4-$[SiH_6]^{2-}$ moiety from **4**-tol, viewed along the Ru-Si-Ru axis. c) Structure of the free $[SiH_6]^{2-}$ dianion as determined by DFT methods.

$[SiH_6]^{2-}$ anion coordinated to two {[PhBP$^{Ph}_3$]Ru} moieties. The six Si–H bonds are indicated by six short Si–H distances (1.69(3)–1.79(4) Å; av. 1.74(4) Å) and three Si–H bonds are coordinated to each ruthenium center (*d*(Ru-H) 1.62(4)–1.73(4) Å; av. 1.68(4) Å). As noted for the structure of **3b**, the Si–H distances measured for **4**-tol would require inaccuracy several times greater than the estimated standard deviation to have true values beyond the range expected for Ru–H–Si bonding, while the Ru–H distances do not indicate obvious systematic errors. Additionally, the measured Si–H distances are intermediate between those determined by XRD for the Ru–H–Si interactions in **2a** (*d*(Si-μ-H) = 1.61(4) and 1.66(4) Å) and **2b**-DMAP (*d*(Si-μ-H) = 1.82(3), 1.98(4), and 1.99(3) Å), which is in agreement with the trend in Si–H bond strength established by FTIR and NMR spectroscopy for this series of related complexes. Interestingly, the Ru–Si distances (*d*(Ru-Si) 2.167(1), 2.168(1) Å) are shorter than those reported for any other ruthenium–silicon compound, a record previously held by [{(*i*Pr$_3$P)$_2$H$_2$Ru}$_2$(η^3,η^3-H$_4$Si)] (*d*Ru–Si = 2.1875(4) Å).[23,26] The two nearly identical Ru–Si distances and approximate D_3 symmetry of **4**-tol suggests that all the Ru–H–Si interactions are equivalent. Each ruthenium center exhibits an octahedral geometry, and the two {[PhBP$^{Ph}_3$]RuH$_3$} fragments are rotated by about 13° from an ideal, staggered conformation (av. P-Ru-Ru-P angle 166.48(3)°). The η^4,η^4-$[SiH_6]^{2-}$ anion exhibits a slight distortion from octahedral geometry, in which the two η^4-H$_3$Si faces are rotated from the staggered conformation (by ca. 13°) and possess H-Si-H angles that are less than 90° (av. 82(2)°; Figure 2b). A fully staggered structure was observed with crystals of **4** grown from benzene (**4**-ben), but the hydride positions in this structure could not be located.

Geometry optimization calculations,[20] starting from the **4**-ben structure with six Ru–H ligands added (*d*Ru–H = 1.6 Å), produced a structure (**4**-DFT) that also exhibits a fully staggered conformation and features Si–H distances (1.767 Å), Ru–H distances (1.743 Å), and Ru–Si distances (2.192 Å) that are similar to those determined by XRD for **4**-tol. The **4**-DFT structure or a slightly twisted version analogous to **4**-tol were determined upon optimization of several different initial starting structures for **4**, including a [{(PhBP$^{Ph}_3$)RuH}$_2${μ-η^3,η^3-H$_4$Si}] structure in which the {[PhBP$^{Ph}_3$]Ru} fragments were in a significantly different initial orientation than those of **4**-DFT. Vibrational analysis of **4**-DFT determined strongly IR active Ru–H stretching modes with frequencies of 1722.23 cm^{-1} and 1731.91 cm^{-1} that are in good agreement with the FTIR data for **4** (1750 cm^{-1}). This confirms that the calculations are accurate with respect to the nature of the Ru–H–Si interactions, which is expected based on the typical accuracy of DFT calculations with regard to transition-metal hydride complexes.[19b,27]

Several resonance structures may be considered for **4**, which depict different levels of Si–H bond cleavage and corresponding levels of Ru→Si back-donation (**A**–**C**; Figure 3).[17] Related [L$_3$MH$_3$SiR$_3$] species that feature short Si–H contacts (*d*(Si–H) 1.86(2)–2.06(4) Å) have been described as M^{IV} silyl complexes with additional M–H···Si interactions (related to structure **B**).[6] The M–H···Si interactions were described in terms of the hydride ligands donating into the Si–R and M–Si σ*-orbitals. If the latter interaction were strong, it would represent a reductive

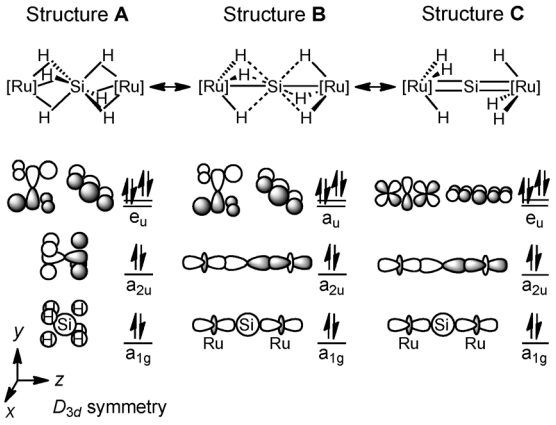

Figure 3. Resonance structures depicting increasing levels of Si–H bond activation in **4**, and the bonding orbitals around silicon corresponding to each resonance structure.

elemination of the three Si–H bonds to give M^{II} structures of the type $[L_3M\{\eta^4\text{-}H_3SiR_3\}]$ (related to structure **A**), but examples of this have never conclusively been shown.[5,6] The resonance structures in Figure 3 feature a similar distinction between a bis-Ru^{II} hexahydridosilicate structure (**A**) and a bis-Ru^{IV} structure featuring two Ru–Si σ-bonds and weaker Ru–H···Si interactions (**B**). Bonding motifs analogous to structure **B** have been reported for structurally related $[\{(R_3P)_3Fe\}_2(\mu\text{-}H)_6B]^+$ complexes[28] and an additional bonding description for **4** features a Ru=Si=Ru core and no Si–H bonding (structure **C**). The short Si–H distances in **4** are consistent with structures **A** or **B** and the short Ru–Si distances and downfield ^{29}Si NMR resonance could indicate Ru=Si character (structure **C**).[26] However, as already noted, the Ru–H stretching frequency and large J_{SiH} values for **4** are characteristic of coordinated Si–H bonds and, thus, strongly support the greater importance of resonance structure **A**. For comparison to **4**, the structure of the hypothetical free $[SiH_6]^{2-}$ anion was determined using DFT methods ($[SiH_6]^{2-}$-DFT; Figure 2c)[20] and displays an octahedral geometry (H-Si-H = 90°) with Si–H distances (1.66 Å) that are somewhat longer than those of silane Si–H bonds (ca. 1.5 Å). The Si–H bonds in **4** are only ca. 0.1 Å longer than those in $[SiH_6]^{2-}$-DFT, which supports structure **A** as the best bonding description for **4**, as each Si–H bond is weakly activated in the η^4,η^4-$[SiH_6]^{2-}$ ligand.

Further support for the importance of structure **A** was found by examining the molecular orbitals for **4**-DFT (Figure 4). The most significant Ru–Si σ-bonding interaction was found in the HOMO−46 orbital, which includes a significant contribution from two ruthenium $4d_{z^2}$ orbitals (9% each) with a smaller contribution from the silicon $3p_z$ orbital (3%). This represents a dative Ru→Si interaction that is consistent with weak back-donation into one of the SiH_6 σ* orbitals, whereas oxidative addition to give structures **B** or **C** should result in two full Ru–Si σ-bonds, formed by interaction of the a_{1g} and a_{2u} linear combinations of ruthenium $4d_{z^2}$ orbitals with the silicon 3s (a_{1g}) and $3p_z$ (a_{2u}) orbitals (Figure 3). The HOMO−179 and HOMO−154 molecular orbitals depict Ru–H–Si bonding interactions that correspond to the a_{1g} and a_{2u} orbitals of structure **A** interacting with a_{1g} and a_{2u} combinations of the ruthenium 5s orbitals. The nearly degenerate HOMO−127 and HOMO−128 also include substantial Ru–H–Si bonding character, which corresponds to the e_u Si–H bonding orbitals in structure **A** interacting with 4d orbitals on ruthenium. These two orbitals resemble the π-bonding orbitals for structure **C** and this may contribute to the relatively downfield ^{29}Si chemical shift for **4**. Further similarity to structure **C** is found in the LUMO and LUMO+1 orbitals of **4**-DFT, which include substantial silicon 3p character and resemble the degenerate π*-LUMOs expected for a Ru=Si=Ru bonding motif. A similar analogy has been noted between the LUMOs of $M(\eta^3\text{-}H_2SiR_2)$, $M(\mu\text{-}H)SiR_2$, and $M(H)_2{=}SiR_2$ complexes and is due to the inability of the hydrogen 1s orbital to contribute to the out of phase combination of the ruthenium 4d orbital with the silicon 3p orbital.[10,29] This also applies to **4**, despite hypercoordination at silicon, and is possible because all six Si–H bonds engage in Ru–H–Si interactions.

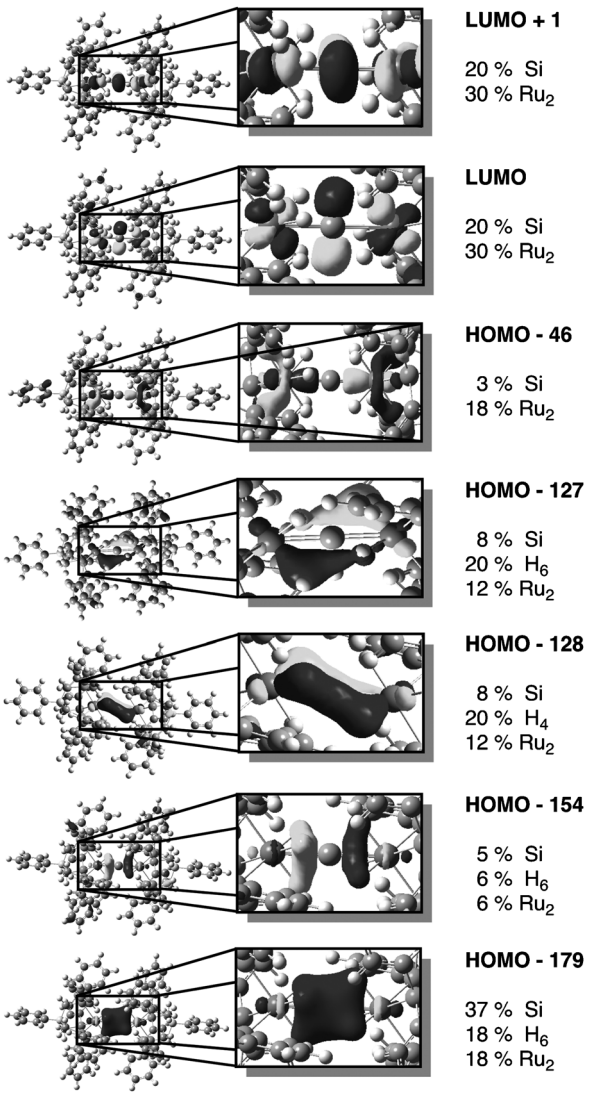

Figure 4. Selected molecular orbitals of **4**-DFT and percent contribution from silicon, the two ruthenium atoms, and six hydride ligands.

The bonding in **4** was also examined using NBO calculations on a slightly modified version of **4**-DFT.[22] The NBO analysis provided a relatively poor bonding description for **4**, which is expected for a highly delocalized structure. However, the NPA and NBO outputs both indicate that each ruthenium has three fairly high occupancy 4d orbitals, consistent with a bis-Ru^{II} description. An NLMO analysis provided a better description of the bonding in **4**, including six nearly identical NLMOs that consist almost entirely of atomic functions on hydrogen (51%), silicon (25%), ruthenium (13%), and phosphorus (8.5%). The only indication of Ru–Si σ-bonding was found in two NLMOs almost entirely composed of ruthenium 4d character (94.5%), with a slight contribution from silicon (3%).

In summary, reactions of primary aryl silanes with **1** or **2** resulted in the formation of novel diruthenium hydridosilicate σ-complexes **3a–c** or **4**, respectively. Complexes **3a–c** feature unique examples of bridging η^3,η^3-$[H_4SiAr]^-$ ligands and are more stable than the only previously isolated $[ArSiH_4]^-$

species, which featured an η^3-$[H_2SiH_2Ph]^-$ ligand in a mononuclear Fe^{II} complex.[4a] Complex **4** is the first isolated compound to include an $[SiH_6]^{2-}$ dianion, which in this case is bound as a bridging η^4,η^4-$[H_6Si]^{2-}$ ligand. This is particularly notable because hydridosilicate dianion σ-complexes had not been conclusively demonstrated, but have been the subject of ongoing discussion.[5,6] The stability of the hydridosilicate anions in **3a–c** and **4** is attributed to the unique ability of the two ruthenium centers in these complexes to uniformly remove electron density from the Si–H bonds.

Received: March 24, 2012
Revised: August 7, 2012
Published online: October 4, 2012

Keywords: hydridosilicates · hypervalent compounds · ruthenium · silicon · σ-complexes

[1] a) R. Criegee, G. Schroder, *Angew. Chem.* **1959**, *71*, 70–71; b) E. O. Fischer, A. Massböl, *Angew. Chem.* **1964**, *76*, 645–645; *Angew. Chem. Int. Ed. Engl.* **1964**, *3*, 580–581; c) D. A. Strauss, R. H. Grubbs, *J. Am. Chem. Soc.* **1982**, *104*, 5499–5500.

[2] a) P. D. Lickiss, *Chem. Soc. Rev.* **1992**, *21*, 271–279; b) S. K. Grumbine, T. D. Tilley, F. P. Arnold, A. L. Rheingold, *J. Am. Chem. Soc.* **1994**, *116*, 5495–5496; c) J. D. Feldman, G. P. Mitchell, J.-O. Nolte, T. D. Tilley, *J. Am. Chem. Soc.* **1998**, *120*, 11184–11185; d) B. K. Campion, R. H. Heyn, T. D. Tilley, *J. Am. Chem. Soc.* **1988**, *110*, 7558–7560; e) T. S. Koloski, P. J. Carrol, D. H. Berry, *J. Am. Chem. Soc.* **1990**, *112*, 6405–6406; f) E. K. Pham, R. West, *J. Am. Chem. Soc.* **1989**, *111*, 7667–7668; g) D. H. Berry, J. H. Chey, H. S. Zipin, P. J. Carrol, *J. Am. Chem. Soc.* **1990**, *112*, 452–453; h) J. M. Dysard, T. D. Tilley, *Organometallics* **2001**, *20*, 1195–1203; i) A. Shinohara, N. Takeda, T. Sasamori, T. Matsumoto, N. Tokitoh, *Organometallics* **2005**, *24*, 6141–6146.

[3] a) M. J. S. Dewar, *Bull. Soc. Chim. Fr.* **1951**, *18*, C71–C79; b) J. Chatt, L. Duncanson, *J. Chem. Soc.* **1953**, 2939–2947.

[4] a) D. V. Gutsulyak, L. G. Kuzmina, J. A. K. Howard, S. F. Vyboishchikov, G. I. Nikonov, *J. Am. Chem. Soc.* **2008**, *130*, 3732–3733; b) T. Y. Lee, L. Dang, Z. Zhou, C. H. Yeung, Z. Lin, C. P. Lau, *Eur. J. Inorg. Chem.* **2010**, 5675–5684.

[5] G. I. Nikonov, *Angew. Chem.* **2001**, *113*, 3457–3459; *Angew. Chem. Int. Ed.* **2001**, *40*, 3353–3355.

[6] a) K. Hübler, U. Hubler, W. R. Roper, P. Schwerdtfeger, L. J. Wright, *Chem. Eur. J.* **1997**, *3*, 1608; b) C. E. F. Rickard, W. R. Roper, S. D. Woodgate, L. J. Wright, *J. Organomet. Chem.* **2000**, *609*, 177–183; c) N. M. Yardy, F. R. Lemke, *Organometallics* **2001**, *20*, 5670–5674; d) M. Möhlen, C. E. F. Rickard, W. R. Roper, D. M. Salter, L. J. Wright, *J. Organomet. Chem.* **2000**, *593*, 458–464; e) K. Hussein, C. J. Marsden, J.-C. Barthelat, V. Rodriguez, S. Conejero, S. Sabo-Etienne, B. Donnadieu, B. Chaudret, *Chem. Commun.* **1999**, 1315–1316.

[7] a) C. Chulte, R. J. P. Corriu, C. Reye, J. C. Young, *Chem. Rev.* **1993**, *93*, 1372–1448; b) R. J. P. Corriu, R. Pen, C. Rayl, *Tetrahedron* **1983**, *39*, 999–1009; c) B. Becker, R. J. P. Corriu, C. Guérin, B. J. L. Henner, *J. Organomet. Chem.* **1989**, *369*, 147–154; d) J. L. Brefort, R. J. P. Corriu, C. Guérin, B. J. L. Henner, *J. Organomet. Chem.* **1989**, *370*, 9–15; e) N. Rot, T. Nijbacker, R. Kroon, F. J. J. de Kanter, F. Bickelhaupt, M. Lutz, A. L. Spek, *Organometallics* **2000**, *19*, 1319–1324.

[8] a) G. Klass, V. C. Trenerry, J. C. Sheldon, J. H. Bowie, *Aust. J. Phys. Chem.* **1981**, *34*, 519–529; b) J. C. Sheldon, R. N. Hayes, J. H. Bowie, *J. Am. Chem. Soc.* **1984**, *106*, 7711–7715; c) D. Hajdasz, R. R. Squires, *J. Am. Chem. Soc.* **1986**, *108*, 3139–3140; d) D. Hajdasz, H. Yeunghaw, R. R. Squires, *J. Am. Chem. Soc.* **1994**, *116*, 10751–10760.

[9] a) R. J. P. Corriu, C. Guérin, B. Henner, Q. Wang, *Organometallics* **1991**, *10*, 2297–2303; b) R. J. P. Corriu, C. Guérin, B. Henner, Q. Wang, *Organometallics* **1991**, *10*, 3574–3581; c) M. J. Bearpark, G. S. McGrady, P. D. Prince, J. W. Steed, *J. Am. Chem. Soc.* **2001**, *123*, 7736–7737; d) P. D. Prince, M. J. Bearpark, G. S. McGrady, J. W. Steed, *Dalton Trans.* **2008**, 271–282.

[10] M. C. Lipke, T. D. Tilley, *J. Am. Chem. Soc.* **2011**, *133*, 16374–16377.

[11] K. Thorshaug, O. Swang, I. M. Dahl, A. Olafsen, *J. Phys. Chem. A* **2006**, *110*, 9801–9804.

[12] a) G. I. Nikonov, *Adv. Organomet. Chem.* **1995**, *53*, 217–309; b) S. Lachaize, S. Sabo-Etienne, *Eur. J. Inorg. Chem.* **2006**, *11*, 2115–2127; c) S. R. Dubberley, S. K. Ignatov, N. H. Rees, A. G. Razuvaev, P. Mountford, G. I. Nikonov, *J. Am. Chem. Soc.* **2003**, *125*, 642–643; d) G. Alcaraz, S. Sabo-Etienne, *Coord. Chem. Rev.* **2008**, *252*, 2395–2409.

[13] C. M. Thomas, J. C. Peters, *Angew. Chem.* **2006**, *118*, 790–794; *Angew. Chem. Int. Ed.* **2006**, *45*, 776–780.

[14] a) J. Y. Corey, J. Braddock-Wilking, *Chem. Rev.* **1999**, *99*, 175–292; b) J. Y. Corey, *Chem. Rev.* **2011**, *111*, 863–1071.

[15] a) D. L. Wilhite, L. Spialter, *J. Am. Chem. Soc.* **1973**, *95*, 2100–2104; b) A. E. Reed, P. R. Schleyer, *Chem. Phys. Lett.* **1987**, *133*, 553–561; c) T. L. Windus, M. S. Gordon, L. P. Davis, L. W. Burggraf, *J. Am. Chem. Soc.* **1994**, *116*, 3568–3579; d) E. P. A. Couzijn, A. W. Ehlers, M. Schakel, K. Lammertsma, *J. Am. Chem. Soc.* **2006**, *128*, 13634–12639.

[16] J. L. Duncan, J. L. Harvie, D. C. McKean, S. Cradock, *J. Mol. Struct.* **1986**, *145*, 225–242.

[17] U. Schubert, *Adv. Organomet. Chem.* **1990**, *30*, 151–187.

[18] F. L. Hirshfeld, *Cryst. Rev.* **1991**, *2*, 169–200.

[19] a) L. Brammer, W. T. Klooster, F. R. Lemke, *Organometallics* **1996**, *15*, 1721–1727; b) M. Grellier, T. Ayed, J. C. Barthelat, A. Albinati, S. Mason, L. Vendier, Y. Coppel, S. Sabo-Etienne, *J. Am. Chem. Soc.* **2009**, *131*, 7633–7640.

[20] Geometry optimization was carried out with Gaussian 09 using the B3PW91 functional and 6-31G(d,p)/LANL 2DZ basis sets.

[21] S. G. Lias, J. E. Bartmess, J. F. Liebman, J. L. Holmes, R. D. Levin, W. G. Mallard, *J. Phys. Chem. Ref. Data* **1988**, *17*, Suppl. 1. All data taken from the NIST Negative Ion Energetics Database, Version 3.00, NIST Standard Reference Database 19B, October **1993**.

[22] NBO 3.0 and NBO 5.0, E. D. Glendening, J. K. Badenhoop, A. E. Reed, J. E. Carpenter, J. A. Bohmann, C. M. Morales, and F. Weinhold, Theoretical Chemistry Institute, University of Wisconsin, Madison (**2001**).

[23] a) I. Atheaux, B. Dannadieu, V. Rodriguez, S. Sabo-Etienne, B. Chaudret, K. Hussein, J.-C. Barthelat, *J. Am. Chem. Soc.* **2000**, *122*, 5664–5665; b) R. B. Said, K. Hussein, J.-C. Barthelat, I. Atheaux, S. Sabo-Etienne, M. Grellier, B. Donnadieu, B. Chaudret, *Dalton Trans.* **2003**, 4139–4146.

[24] K. Puhakainen, D. Benson, J. Nylén, S. Konar, E. Stoyanov, K. Leinenweber, U. Haussermann, *Angew. Chem.* **2012**, *124*, 3210–3214; *Angew. Chem. Int. Ed.* **2012**, *51*, 3156–3160.

[25] M. D. Curtis, P. S. Epstein, *Adv. Organomet. Chem.* **1981**, *19*, 213–255.

[26] A search of the Cambridge Structure Database, as of 2012, found that structurally characterized Ru=Si bonds fall in the range 2.181(1)–2.2842(5) Å: a) see ref [2b]; b) M. Ochiai, H. Hashimoto, H. Tobita, *Angew. Chem.* **2007**, *119*, 8340–8342; *Angew. Chem. Int. Ed.* **2007**, *46*, 8192–8194; c) A. Takaoka, A. Mendirata, J. C. Peters, *Organometallics* **2009**, *28*, 3744–3753; d) H. Hashimoto, J. Sato, H. Tobita, *Organometallics* **2009**, *28*, 3963–3965; e) P. G. Hayes, R. Waterman, P. B. Glaser, T. D. Tilley, *Organometallics* **2009**, *28*, 5082–5089.

[27] F. Maseras, A. Liedós, E. Clot, O. Eisenstein, *Chem. Rev.* **2000**, *100*, 601 – 636.
[28] a) D. G. Gusev, R. Hübener, P. Burger, O. Orama, H. Berke, *J. Am. Chem. Soc.* **1997**, *119*, 3716 – 3731; b) A. C. Hillier, H. Jacobsen, D. Gusev, H. W. Schmalle, H. Berke, *Inorg. Chem.* **2001**, *40*, 6334 – 6337; c) G. Guilera, G. S. McGrady, J. W. Steed, N. Kaltsoyannis, *New J. Chem.* **2004**, *28*, 444 – 446.
[29] V. M. Iluc, G. L. Hillhouse, *J. Am. Chem. Soc.* **2010**, *132*, 11890 – 11892.
[30] CCDC 900947 (**3a**), CCDC 900948 (**3b**), CCDC 900949 (**4**-tol), and CCDC 900950 (**4**-ben) contain the supplementary crystallographic data for this paper. These data can be obtained free of charge from The Cambridge Crystallographic Data Centre via www.ccdc.cam.ac.uk/data_request/cif.

